The Journal of Experimental Biology 207, 841-852
Published by The Company of Biologists 2004
doi:10.1242/jeb.00839

Sodium and potassium currents of larval zebrafish muscle fibres

Steven D. Buckingham and Declan W. Ali*

Department of Biological Sciences, University of Alberta, CW-405 Biological Sciences Building, Edmonton, Alberta, T6G 2E9, Canada

*Author for correspondence (e-mail: declan.ali@ualberta.ca)

Accepted 15 December 1003

Summary

The steady-state and kinetic properties of Na^+ and K^+ currents of inner (white) and outer (red) muscles of zebrafish larvae 4–6 days post-fertilization (d.p.f.) are described. In inner muscle, the outward currents were half-activated at –1.0 mV and half-inactivated at –30.4 mV, and completely inactivated within 100 ms of depolarization. The inward currents of inner fibres were half-activated at –7.3 mV and half-inactivated at –74.5 mV and completely inactivated within 5 ms of depolarization. Inner muscle fibres were found to support action potentials, while no action potentials could be evoked in outer muscles. In inner muscle fibres, all tested levels of depolarizing current above a threshold value evoked only one action potential. However, spiking at frequencies of up to 200 cycles s^{-1} was evoked by the injection of depolarizing pulses separated by short hyperpolarizing currents. We suggest that the properties of the inward sodium and outward potassium currents permit high frequency firing in response to a pulsatile depolarizing input of the kind expected in fast swimming, whilst safeguarding against tetany during a strong depolarization.

Key words: zebrafish, *Danio rerio*, muscle, sodium current, potassium current, action potential.

Introduction

The excitability of muscle cells is shaped in part by the properties of voltage-gated Na^+, K^+ and Ca^{2+} channels (Sanes and Lichtman, 1999; Hille, 2001; Armstrong and Hille, 1998). Like neuronal channels, skeletal muscle Na^+ channels are complexes of α and β subunits, except that they are composed of only one β subunit rather than two (Catterall, 1992; Goldin, 2001; Isom et al., 1995). The properties of muscle-specific, voltage-dependent Na^+ channels have been investigated in a variety of preparations (O'Leary, 1998; Lerche et al., 1996; Ruff, 1996; Almers et al., 1984; Adrian and Marshall, 1977; Duval and Leoty, 1978; Stanfield, 1972). All appear to be typical Na^+ channels that rapidly activate and inactivate within a few milliseconds, although they differ in their V_{50} values for activation and inactivation (O'Leary, 1998). Muscle Na^+ channels differ from their neuronal counterparts in that they are blocked by ω-conotoxin, which has little effect on neuronal Na^+ channels (Cruz et al., 1985; Moczydlowski et al., 1986).

K^+ channels associated with muscle fibres have been described from rat (Duval and Leoty, 1980a,b) and frog (Camacho et al., 1996). An inactivating, outward K^+ current exists in both rat and frog skeletal fibres, while a non-inactivating outward K^+ current is associated with rat slow-twitch muscle (Duval and Leoty, 1980a,b).

The zebrafish *Danio rerio* offers many advantages for investigating the relationship between ion channel expression and muscle fibre activity *in vivo*. In particular, the ready accessibility of the developing motor system to currently available electrophysiological techniques, the availability of a large number of viable mutants, and the ease of recording from both red (outer) and white (inner) muscle fibres, make this preparation particularly attractive for investigating differences in ion channel expression on physiologically different fibre types in developing animals (Drapeau et al., 2002).

As in most other teleosts, zebrafish axial muscle comprises both red and white fibre types (Greer-Walker and Pull, 1975). In the embryo and larva, these have been shown to perform different roles in swimming (Buss and Drapeau, 2002), with red fibres being derecruited at faster fictive swimming rates and white fibres probably being inactive during slow swimming (Buss and Drapeau, 2002). Although the development of two cell types (red and white fibres) with distinct behavioural roles in the developing zebrafish axial muscle system offers a convenient model in which to examine the differentiation of electrical phenotypes, to date the electrophysiology of larval zebrafish muscle has received surprisingly little attention.

Based on voltage recordings of embryonic and larval red and white fibres, an initial study (Buss and Drapeau, 2000) concluded that the development of both red and white fibres was similar, but not identical. Neither cell type was reported to exhibit action potentials, and both types were found to be able to follow trains of pulsatile electrical stimulation at up to 30 Hz (Buss and Drapeau, 2000). This raises the question of

how excitation–contraction coupling occurs in the absence of muscle action potentials.

Here we use whole-cell, patch-clamp (under voltage-clamp and current-clamp modes) to determine the kinetic and steady state properties of voltage-gated ion currents of larval axial red and white muscle. Embryos undergo a characteristic developmental sequence of motor behaviours that starts with spontaneous alternating trunk contractions (17–30 h post fertilization; h.p.f.), followed by the emergence of coiling in response to touch (21–27 h.p.f.), and finally by active swimming in response to touch (after 27 h.p.f.) (Saint-Amant and Drapeau, 1998). We investigated trunk muscles in zebrafish 4–6 days post fertilization (d.p.f.), since at this age the larvae exhibit mature locomotor behaviours (Plaut, 2000; Saint-Amant and Drapeau, 1998). This is the first step in a larger study aimed at determining how developmental changes in ion channel expression affect spiking parameters of maturing muscle cells. Here we report for the first time in this species, that inner (white) muscles support action potentials while the outer (red) muscles do not. Interestingly, inner white muscles were found to be capable of generating only one action potential in response to sustained depolarizations beyond threshold. We propose that this characteristic serves as a mechanism whereby inner muscle sustains once-only firing during swimming whilst preserving the capacity for high frequency firing in response to periodic neuronal stimulation.

Materials and methods

Preparation

Adult male and female zebrafish *Danio rerio* L. were obtained from a breeding facility (Carolina Biological Supply Co., Burlington, NC, USA) and maintained according to established procedures (Westerfield, 1995). All procedures were carried out in compliance with the guidelines stipulated by the Canadian Council for Animal Care and the University of Alberta. Embryos and larvae were raised at 28.5°C. Larvae were anesthetized in 0.02% tricaine (MS-222; Sigma Chemical, St Louis, MO, USA) in recording solution before and during dissections. The preparation was pinned through the notochord into a Sylgard-lined dish, and a pair of fine forceps (Dumont #5; Fine Science Tools, Vancouver, BC, Canada) was used to remove the skin overlaying trunk segments, thus exposing the trunk musculature. The preparation was decapitated with a fine pair of forceps and then immediately moved to the recording chamber and continually perfused with recording solution containing d-tubocurarine (15 μmol l^{-1}) but not tricaine. The compositions of the recording solutions depended upon the type of ionic current to be isolated, and are described in Table 1. Inner and outer muscle cells were easily distinguished under Nomarski Differential Interference Contrast (DIC) optics (Fig. 1A,B). The outer layer of muscle fibres run parallel to the notochord, whereas the inner muscle fibres, one layer deep, run at an oblique angle, approximately 30–40° tangential to the notochord (Fig. 1). Outer and inner muscles from musculature dorsal and ventral to the midline were studied. The data recorded from dorsal and ventral musculature were similar and were therefore subsequently pooled.

Electrophysiology

Glass pipettes were prepared from borosilicate glass (GC150T, World Precision Instruments, Sarasota, FL, USA), pulled on a P-97 pipette puller (Sutter Instrument Co., Novato, CA, USA) and fire polished (Micro-Forge MF-830; Narishige, Japan) to a resistance of 0.5–2 MΩ. Signals were amplified using an Axopatch 200B (Axon Instruments, Foster City, CA, USA) and displayed on an IBM-compatible PC using pClamp 8.02 software (Axon Instruments) and on a digital oscilloscope (TDS 220; Tektronix, Beaverton, OR, USA). Immediately after the establishment of the whole-cell mode (Hamill et al., 1981), series resistance was compensated by at least 80%, and usually by 90%, using the amplifier's compensation circuitry. Experiments were aborted if the series resistance changed by more than 15%. Data were sampled at 50 kHz using a Digidata 1322A (Axon Instruments) analogue to digital converter, or at 250 kHz when recording Na^+ currents. Data were analyzed using Clampfit 8.0 software (Axon Instruments) and plotted using SigmaPlot 7.0 (SPSS). Capacitative and leak currents were subtracted on-line using the P/N protocol provided with pClamp 8.02, in which we used 4 depolarizing pulses.

Table 1. *Salines and pipette-filling solutions*

Saline	NaCl	ChoCl	KCl	CsCl	$CaCl_2$	$CdCl_2$	$MgCl_2$	BAPTA	Hepes	Glucose
Extracellular saline										
Normal	118	–	2.9	–	0.7	–	10	–	10	10
Na^+-isolating	118	–	–	2.9	–	0.7	10	–	10	10
K^+-isolating	–	134	2.9	–	–	0.7	10	–	10	10
Pipette-filling solution*										
Normal	–	–	134	–	–	–	4	10	10	–
Na^+-isolating	–	–	–	130	–	2	4	10	10	–
K^+-isolating	–	–	124	–	–	2	4	10	10	–

All values are mmol l^{-1}.
*Na_2ATP (4 mmol l^{-1}) and LiGTP (0.4 mmol l^{-1}) were added to all pipette-filling solutions.

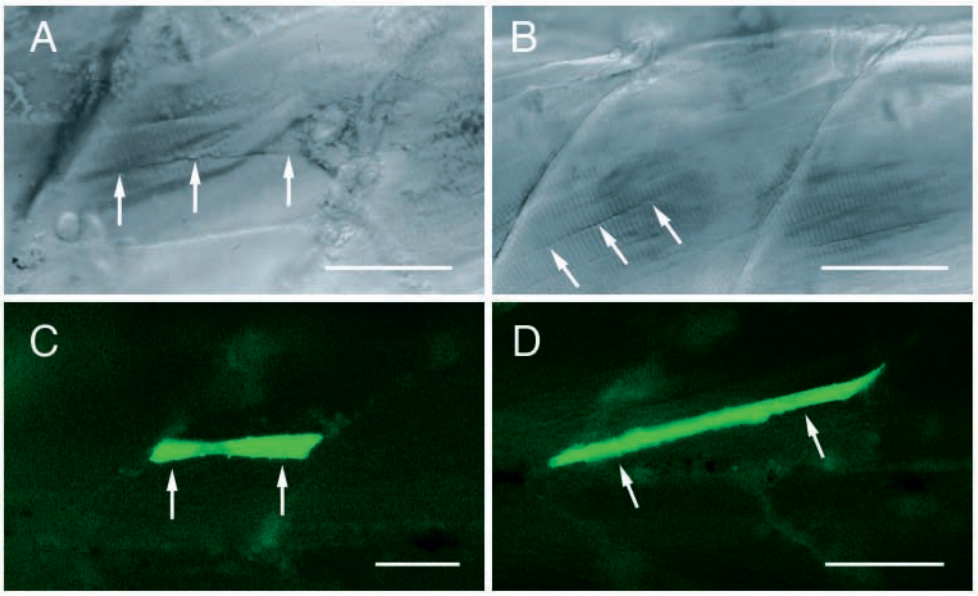

Fig. 1. (A,B) Nomarski Differential Interference Contrast (DIC) images of larval zebrafish outer, red (A) and inner, white (B) muscle fibres. The outer, red fibres constitute a single, superficial cell layer and run parallel to the notochord, while the inner, white fibres are several cell layers thick and run obliquely to the notochord and midline. (C,D) Individual red (C) and white (D) muscle fibres from 5 d.p.f. larvae filled with Lucifer Yellow (0.1%) in the presence of 1-heptanol (2 mmol l^{-1}). Arrows point to the edges of the muscle fibres. Scale bars, 50 μm.

Salines and pipette-filling media

Salines and pipette-filling media were prepared as in Table 1. The pH of all extracellular solutions was adjusted to 7.8 with NaOH or KOH depending upon the experiment, while the pH of all intracellular solutions was adjusted to 7.6 with CsOH or KOH. The final osmolarity of all solutions was adjusted to 290±2 mOsm l^{-1}. Pipette filling solutions were supplemented with Na_2ATP (4 mmol l^{-1}) and LiGTP (0.4 mmol l^{-1}).The pipette-filling solutions for the current-clamp experiments consisted of either the 'Normal' solution (Table 1) or a low Cl^- solution composed of the following: 140 mmol l^{-1} D-gluconic acid K^+ salt, 6 mmol l^{-1} KCl, 4 mmol l^{-1} $MgCl_2$, 10 mmol l^{-1} EGTA, 10 mmol l^{-1} Hepes, 4 mmol l^{-1} Na_2ATP and 0.4 mmol l^{-1} LiGTP. 1-Heptanol (2 mmol l^{-1}) was added to the extracellular saline for the voltage-clamp experiments in order to block gap junctions and reduce electrical coupling between cells (Nguyen et al., 1999; Saint-Amant and Drapeau, 2000).

All solutions and drugs were bath-applied at a flow rate of 2 ml min^{-1}. All drugs were acquired from Sigma, unless otherwise indicated.

Results

Voltage-clamp recordings were taken from outer and inner muscles (Fig. 1) of 4–6 d.p.f. zebrafish larvae, which at this age display mature motor behaviours. Over this age range, we found no difference in the steady-state and kinetic properties of either Na^+ or K^+ currents other than the absolute amplitude of the currents. We therefore plotted all currents in current–voltage plots as specific current (pA) per pF of cell membrane capacitance, as read from the compensating circuitry of the amplifier.

Fire-polished glass patch pipettes readily formed high-impedance (GΩ) seals with both inner and outer muscle fibres, and the whole-cell patch-clamp configuration was achieved either by application of negative pressure or by a combination of negative pressure and a brief depolarizing current. Most cells recorded in the whole-cell patch clamp mode had input resistances of less than 80 MΩ, although many cells had markedly higher input resistances (more than 300 MΩ; Table 2). Because many of the currents recorded in these experiments had amplitudes to the order of 10 nA for white fibres and 4 nA for red fibres, this study included only those

Table 2. *Values of fibre parameters*

Fibre type	R_s (MΩ)	R_m (MΩ)	Cap (pF)	% compensation
Red fibres				
Normal saline	2.9±0.2 (8)	221±37 (8)	27.9±1.7 (8)	80–90
Na^+-isolating saline	2.7±0.2 (5)	615±214 (5)	37.0±8.3 (5)	80–90
K^+-isolating saline	3.1±0.2 (8)	604±62 (8)	28.5±0.8 (8)	80–90
White fibres				
Normal saline	2.3±0.2 (10)	67±6 (10)	59.0±7.9 (10)	80–90
Na^+-isolating saline	2.3±0.3 (7)	127±24 (7)	71.9±7.6 (7)	80–90
K^+-isolating saline	2.9±0.4 (8)	74±9 (8)	59.9±3.6 (8)	80–90

Values are means ± S.E.M. (*N*).
R_s, series resistance; R_m, membrane resistance; Cap, membrane capacitance.

cells in which the ratio of the input resistance to the access resistance (both estimated electronically by the data acquisition software) exceeded 10 both before and after recordings. The large size of the muscle fibres coupled with series resistance will introduce errors in voltage control of the fibres (Penner, 1995). We calculated that the compensated series resistance results in a maximum voltage error for red fibres on the order of approximately 1–2 mV, while for white fibres the error is approximately 3–5 mV. In addition, series resistances ranging from 2.7 to 3.1 MΩ for recordings from red fibres, and membrane capacitance values of 28–37 pF (Table 2) results in membrane-charging time constants ($\tau=R_s\times Cm$) to the order of 12–15 μs after ~85% compensation, whereas for white fibres the time constant ranges between 20 and 26 μs.

To ensure that we recorded from only individual muscle fibres, we included the gap junction blocker 1-heptanol (2 mmol l^{-1}) in the exctracellular saline in order to uncouple the muscle fibres (Nguyen et al., 1999). When Lucifer Yellow (0.1%) was included in the pipette, only individual fibres were stained in the presence of 1-heptanol (Fig. 1C,D), suggesting that the presence of the alcohol effectively isolated the cells.

Currents of outer and inner muscle

When all major ions (Na^+, K^+, Ca^{2+} and Cl^-) were present in the saline and in the pipette-filling medium, depolarizations

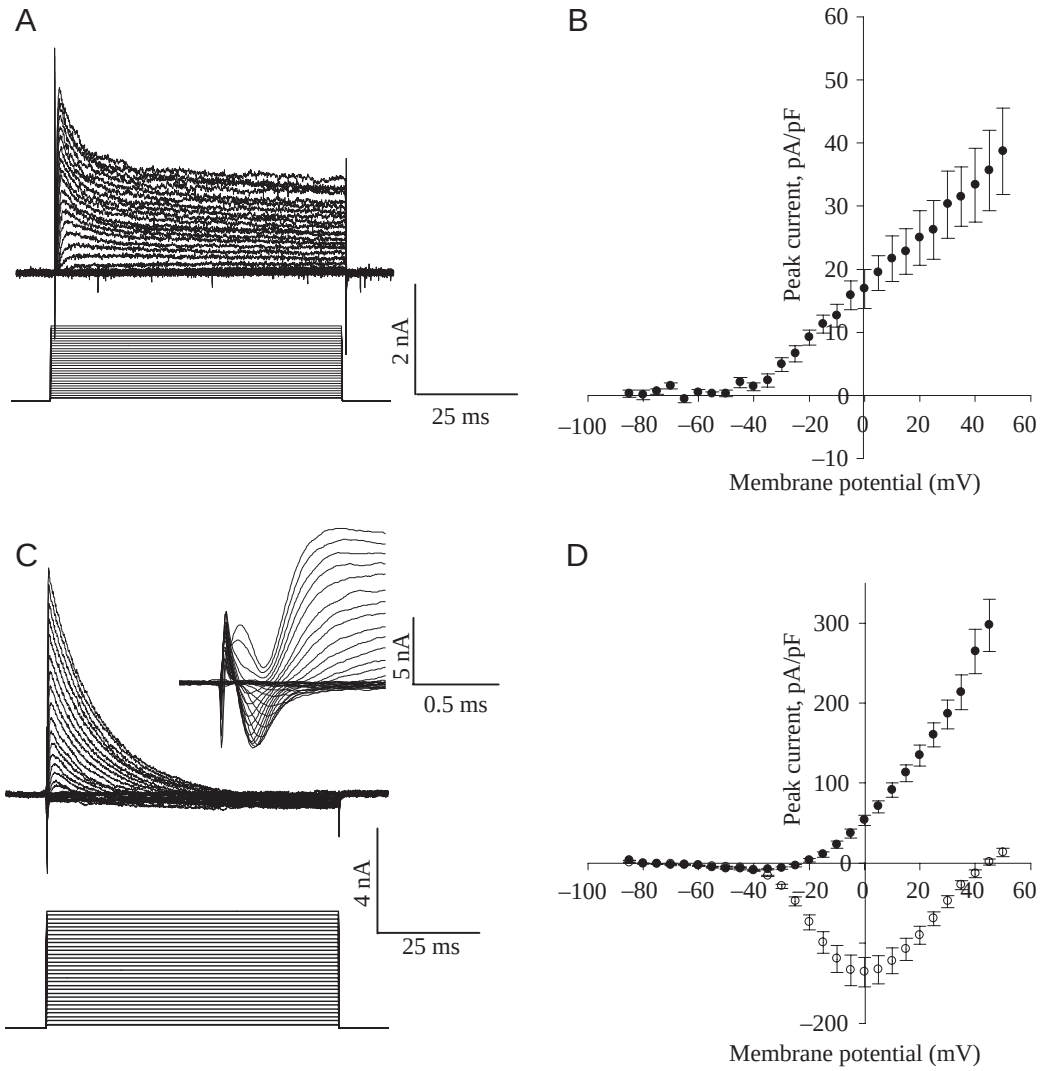

Fig. 2. Voltage-gated currents recorded from outer (A,B) and inner (C,D) muscle of 4–6 d.p.f. zebrafish larvae in normal physiological saline (Na^+, K^+, Ca^{2+} and Cl^- present). (A) Stepwise, 100 ms depolarizations from a range of potentials –85 to +50 mV (at 5 mV intervals) from a holding potential of –90 mV give rise to almost exclusively outwardly directed currents in voltage-clamped, outer muscle fibres. These currents show some evidence of an inactivating component. (B) Currents are evoked at potentials more positive to around –40 mV, and continue to increase with more depolarized potentials. (C) Similar voltage protocols applied, using the same salines, to inner zebrafish muscle evoke a pronounced, brief inward current (inset) followed by outwardly directed currents with a strong inactivating component. Current–voltage plots (D) of the peak amplitudes of the inward and outward currents reveal that inward currents are evoked at potentials more positive to around –40 mV, and outward currents more positive to around –20 mV. Filled symbols, outward currents; open symbols, inward currents.

of voltage-clamped fibres evoked outward currents in outer muscle (Fig. 2A) and both inward and outward currents in inner muscle (Fig. 2C). In outer muscles, stepwise, 100 ms depolarizations from a range of potentials from –85 to +50 mV (at 5 mV intervals) from a holding potential of –90 mV gave rise to outwardly directed currents with some evidence of an inactivating component at greater levels of depolarization (Fig. 2A). Inwardly directed currents were not visible in these recordings. Plotting the peak amplitudes of the outward currents against the amplitude of the depolarizing step revealed that currents were evoked at potentials more positive to around –40 mV, and continued to increase with more depolarized potentials (Fig. 2B).

In contrast, similar voltage protocols applied to inner muscle evoked a pronounced, brief inward current followed by outwardly directed currents with a strong inactivating component (Fig. 2C and inset). Current–voltage plots (Fig. 2D) of the peak amplitudes of the inward and outward currents revealed that the inward current was evoked at membrane potentials more positive to around –40 mV, and the outward at potentials more positive to –20 mV.

Na^+ currents of inner muscle

Putative Na^+ currents were isolated from inner muscle by performing voltage-clamp recordings in saline in which all the potassium ions were replaced by equimolar cesium ions, all the calcium ions replaced with equimolar cadmium ions, and BAPTA added to the intracellular medium to 10 mmol l^{-1} to reduce twitching (Table 1). The addition of BAPTA to the pipette medium prevented contractions in inner muscle, but not in outer muscle. Under these recording conditions, stepwise, 5 ms depolarizations from a holding potential of –90 mV to a range of potentials from –90 to +70 mV evoked rapidly activating and rapidly inactivating, inwardly directed currents (Fig. 3B, inset) up to 10 nA in amplitude. These currents appeared in response to potentials more positive than about –40 mV and reversed at +48±3.7 mV (N=8). When similar protocols were applied to voltage-clamped outer muscle fibres using the same recording conditions, no currents greater than 0.5 nA were observed (Fig. 3A) in any of the five cells tested.

Steady state properties of Na^+ currents

Steady-state activation and inactivation properties were determined for Na^+ currents of inner muscle fibres (Fig. 3C). The voltage-dependence of steady-state activation was determined by first measuring the reversal potential for each set of *I–V* traces (such as those summarized in Fig. 3B) and then measuring the ratio of the peak current at each potential to the driving force (estimated as the difference between the potential and the reversal potential). This ratio, which is the

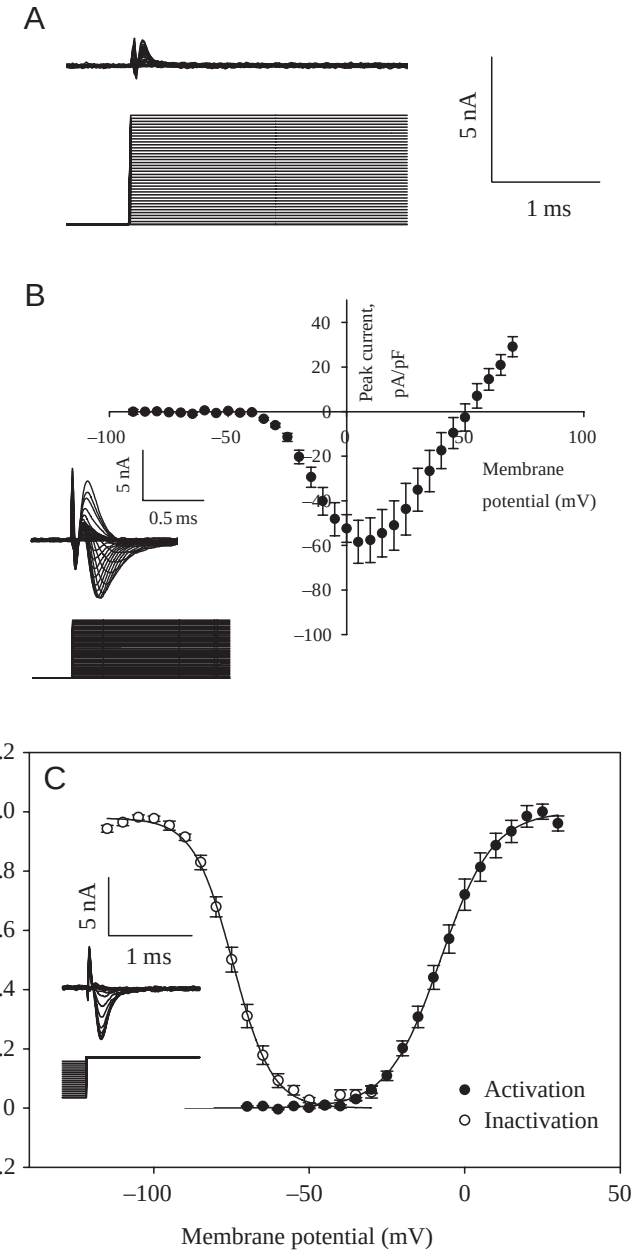

Fig. 3. Isolation of Na^+ currents of 4–6 d.p.f. zebrafish outer (A) and inner (B,C) muscle. In these experiments, Na^+ currents were isolated by performing voltage-clamp recordings in saline in which all the potassium ions were replaced by equimolar cesium ions, and all the calcium ions replaced with equimolar cadmium ions, with BAPTA (10 mmol l^{-1}) supplementing the intracellular medium. (A) Stepwise, 5 ms depolarizations fail to elicit inward, Na^+ currents in outer muscle. (B,C) Stepwise, 5 ms depolarizations from a holding potential of –90 mV to a range of potentials from –85 to +30 mV evoked rapidly activating and rapidly inactivating, inwardly directed currents (inset), which appeared at potentials more positive than about –40 mV and reversed around +50 mV. Values are means ± S.E.M. of 8 experiments on separate muscle fibres. (C) Steady state activation and inactivation of Na^+ currents recorded from inner muscle. Values are means of 12 (activation) and 9 (inactivation) separate experiments ± S.E.M. The data thus derived for both activation and inactivation were then fitted to a Boltzmann function giving estimated values of V_{50} of activation of –7.3±1.6 mV and slope 8.4±0.5 mV/e (N=12) and V_{50} of inactivation of –74.5±1.1 mV and slope of –6.0±0.2 mV/e (N=9). See text for details.

estimated conductance, plotted against the amplitude of the depolarizing pulse, yielded a saturating curve that, when normalized to the maximum values, was fitted to a Boltzmann equation of the form:

$$A = 1/\{1 + e[(V–V_{50})/b]\} , \quad (1)$$

where A is the activation variable (the proportion of available channels open), V is the potential of the depolarizing pulse, V_{50} is the potential of half activation and b is the Boltzmann slope factor. This gave a value for V_{50} of –7.3±1.6 mV, and slope factor of 8.4±0.5 mV/e, N=12.

Steady-state inactivation was determined by measuring the amplitude of depolarization-evoked currents following a preconditioning period. A series of 50 ms depolarizations from a holding potential of –100 mV to a range of potentials from –115 to –10 mV in 5 mV steps was followed by a 5 ms step to –5 mV to evoke the inward current (Fig. 3C, inset). The ratio of the amplitude G of the inward currents to the maximum amplitude G_{max} was plotted against the membrane potential during the preconditioning step. The data thus derived were then fitted to a Boltzmann function, which yielded an estimated value of V_{50} of inactivation of –74.5±1.1 mV and slope of –6.0±0.2 mV/e, N=9.

Inactivation kinetics of Na^+ currents of inner muscle

The time constants of inactivation and the voltage-dependence of recovery from inactivation of Na^+ currents of inner muscle were determined. To derive the time constant of inactivation, the decaying phases of Na^+ currents illustrated in Fig. 3B were each fitted to a single exponential, the time constant τ (ms) of which was plotted against the amplitude of the depolarizing pulse. The rate of inactivation was found to be strongly voltage-dependent (Fig. 4A) and could be described by the function:

$$\tau_{inact} = 0.08 + 0.009e^{-0.14V} , \quad (2)$$

where (N=9), V is the membrane potential and τ_{inact} is the time constant of inactivation.

The rate of recovery of inactivation was measured using a paired pulse protocol. A 5 ms depolarizing step to 20 mV was

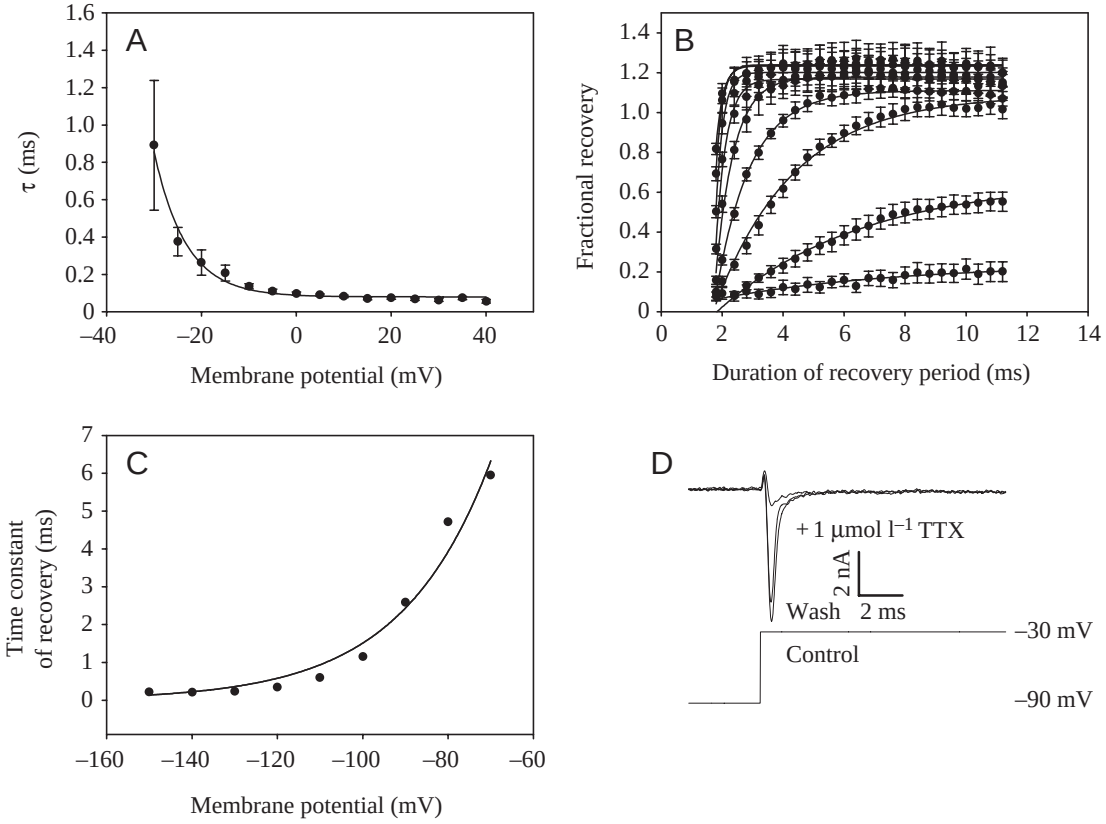

Fig. 4. Time constants of inactivation and voltage-dependence of recovery from inactivation of Na^+ currents of inner muscle. (A) The decaying phase of Na^+ currents illustrated in Fig. 3B were fitted to single exponentials and the time constants τ plotted against the amplitude of the depolarizing pulse. The rate of inactivation can be seen to be strongly voltage-dependent. (B) The rate of recovery of inactivation was measured using a paired two-pulse protocol. A 5 ms depolarization to 20 mV was applied to completely inactivate the Na^+ currents. This was then followed by a 0.5–9 ms recovery step to one of a range of potentials (from –70 to –150 mV in 10 mV steps). The amplitude of currents evoked by a second test pulse (of identical duration and amplitude to the first) was plotted against the duration of the recovery period. The data thus derived were fitted to a single exponential function, the estimated time constants of which were plotted against the membrane potential of the recovery period (C), revealing a strong voltage dependence of the rate of recovery of inactivation. (D) The inward currents observed in Na^+-isolating salines are blocked by the application of micromolar concentrations of TTX, confirming their identity as Na^+ currents.

applied to completely inactivate the Na^+ currents, followed by a 0.5–9 ms recovery step to allow partial recovery of the currents. A second test pulse, of identical form to the first, was applied to determine the proportion of currents that had recovered. The ratio of the amplitudes of currents evoked by the first and second test pulses was plotted against the duration of the recovery period. The data thus obtained at different interstimulus potentials (from –70 to –150 mV in 10 mV steps) could best be fitted to simple, single exponential functions (Fig. 4B), which serve as estimates of the time-constant of recovery from inactivation. Plotting these time constants against the interstimulus potential (Fig. 4C), revealed that the rate of recovery of inactivation was strongly voltage-dependent, and could be described by the function

$$\tau_{recov} = 180e^{0.048V}, \quad (3)$$

where V is the membrane potential and τ_{recov} is the time constant of recovery from inactivation.

The inward currents observed in Na^+-isolating salines were reversibly blocked by the application of micromolar concentrations of TTX (1 μmol l^{-1}; Fig. 4D) and reversed near the equilibrium potential for sodium ions calculated from the sodium ion concentrations using the Nernst equation, suggesting that they are carried by sodium ions.

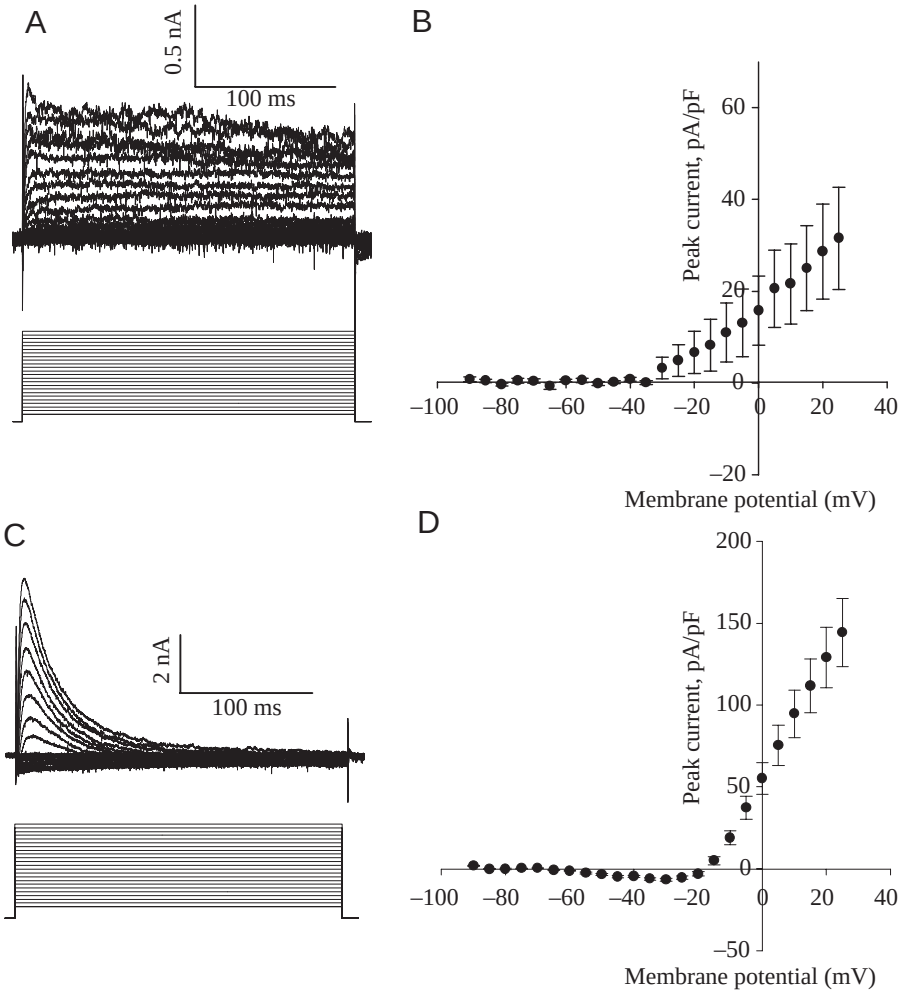

Fig. 5. Isolation of K^+ currents from inner and outer muscle of 4–6 d.p.f. zebrafish larvae was performed by applying depolarizing pulses to voltage-clamped fibres in saline in which all sodium ions were replaced with equimolar choline ions and all calcium ions were replaced with equimolar cadmium ions and supplemented with BAPTA (10 mmol l^{-1}). (A) K^+ currents of outer muscle. A series of 250 ms depolarizations from a holding potential of –100 mV to a range of potentials from –95 to 25 mV evoked outwardly directed currents with little or no evidence of inactivation. (B) A current–voltage plot of such currents shows that they appear at membrane potentials more positive to around –40 mV and increase with more positive potentials. (C) K^+ currents of inner muscle. (D) The current–voltage plot of these currents reveals that they are activated at potentials more positive than around –20 mV. There is still some residual inward current. Values are means ± S.E.M. of at least eight separate experiments

K^+ currents of inner and outer muscle

Isolation of K^+ currents of inner and outer muscle of 4–6 d.p.f. zebrafish larvae was accomplished by applying depolarizing pulses to voltage-clamped fibres using saline and pipette media in which all sodium ions were replaced with equimolar choline ions, all calcium ions replaced with equimolar cadmium ions and BAPTA added to the intracellular medium to 10 mmol l^{-1}. The use of high concentrations of potassium ions in the pipette appeared to compromise the health of the fibres, as determined by seal and input resistances and by the rapid deterioration of whole cell recordings, especially in the case of outer fibres. However, high-quality recordings could be obtained from these cells in sufficient numbers. K^+ currents recorded in outer muscle in response to a series of 250 ms depolarizations imposed from a holding potential of –100 mV to a range of potentials from –95 to 25 mV showed little or no evidence of inactivation (Fig. 5A). These currents appeared at membrane potentials more positive to around –40 mV and increased as the depolarizing potentials were made more positive (Fig. 5B; N=8). Similar protocols applied to inner muscle evoked outwardly directed currents that were of larger amplitude than those of outer muscle, and that inactivated rapidly and completely (Fig. 5C). Current–voltage plots of the peak amplitudes of these currents revealed that the currents were activated at potentials more positive than around –20 mV, and that there remained some residual inward current (Fig. 5C,D; N=8).

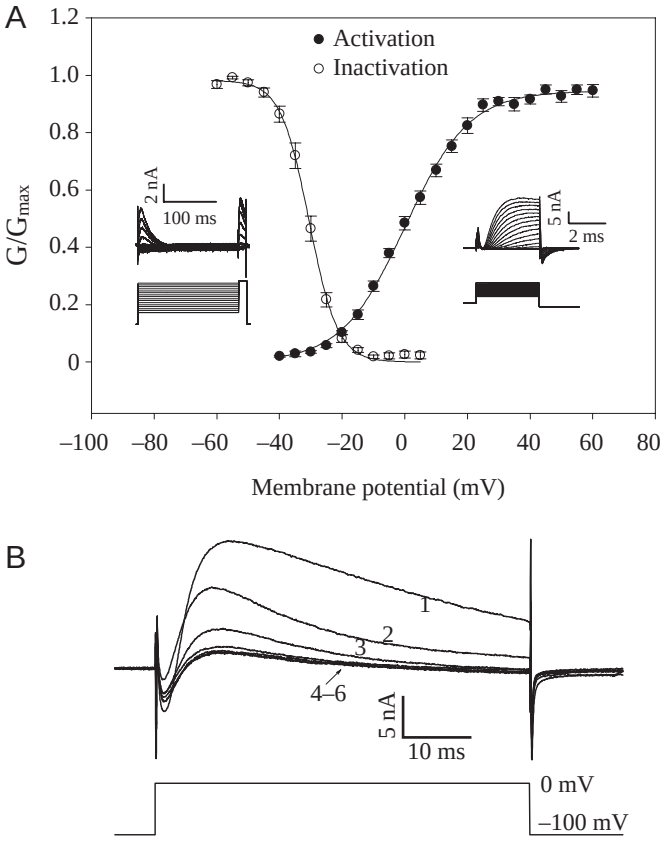

Fig. 6. (A) Steady-state activation and inactivation of putative K^+ currents of 4–6 d.p.f. zebrafish inner muscle. Steady-state activation (filled circles; *N*=7) was determined by applying a series of 5 ms activating pulses from a holding potential of –100 mV to a range of potentials from –45 to +65 mV at 5 mV intervals (inset, right). These pulses were followed immediately by a step to –130 mV to enable the measurement of tail currents. The amplitudes of the tails were normalised to a maximum value of 1 and plotted against the amplitude of the activating pulse. Steady state inactivation (open circles; *N*=6) was determined as in Fig. 3C (inset, left). (B) These outwardly directed currents are blocked by 10 μmol l^{-1} 4-aminopyridine (4AP) in a use-dependent manner. Stepwise 250 ms depolarizations from a holding potential of 100 mV to a potential of 0 mV were applied as the larva was perfused in saline containing 10 μmol l^{-1} 4AP. Numbers indicate the sequence of depolarizing pulses.

Steady-state activation and inactivation of K^+ currents

Steady-state activation and inactivation of putative K^+ currents of inner muscle were determined. Steady-state activation was estimated from isochronal isopotential tails, thereby eliminating errors introduced by estimating the reversal potential of the putative K^+ currents since the measurements are made at the same potential. A series of 5 ms activating pulses from a holding potential of –100 mV to a range of potentials from –45 to +65 mV at 5 mV intervals (Fig. 6A, right inset) were applied. These pulses were followed immediately by a step to –130 mV to enable the measurement of tail currents, which at this potential are slower and therefore easier to measure. The amplitudes of the tails were normalized to a maximum value of 1 and plotted against the amplitude of the activating pulse (Fig. 6A). These data were fitted to a Boltzmann function giving an estimated V_{50} of activation of –1.03±1.02 mV, *N*=7 and slope factor of 10.82±0.48 mV/e, *N*=7.

Steady state inactivation was determined using similar protocols as for Na^+ currents (Fig. 6A, left inset). A 250 ms conditioning pulse was followed immediately by a 20 ms test pulse to 10 mV. The peak amplitude of the response to the test pulse was normalized to a maximum value of 1 and minimum value of 0 and plotted against the conditioning membrane potential (Fig. 6A, open circles). These data could be fitted to a Boltzmann function giving a V_{50} of inactivation of –30.4±0.9 mV, *N*=8 and slope factor of –4.4±0.1 mV/e, *N*=8.

These outwardly directed currents were blocked by continual bath perfusion of 10 μmol l^{-1} 4-aminopyridine (4AP) (Fig. 6B) Stepwise, 50 ms depolarizations from a holding potential of –100 mV to a potential of 0 mV evoked outward currents regardless of how long the preparation had been exposed to 4AP, even after other fibres had previously been tested in 4AP. Responses to subsequent depolarizing pulses, however, were progressively smaller (Fig. 6B). The rate of decline in amplitude was independent of the interval between the pulses, and was a function of the number of previous pulses, indicating that the block by 4AP is use-dependent.

Action potentials in inner muscle

Using the patch-clamp amplifier in current-clamp mode, action potentials were recorded from inner muscle in response to injected current. The Axopatch 200B patch clamp amplifier is not ideally suited for accurately recording the true kinetics of an action potential, and tends to distort the action potential waveform (Magistretti et al., 1996). However, since it was our intention to record the occurrence of action potentials without regard to precise details of their waveforms, we used the Axopatch 200B in current-clamp mode accepting that there would unavoidably be errors associated with the shape of the action potential.

Two different pipette-filling solutions were used. One was the ‘Normal’ solution that we used to voltage-clamp the fibres when investigating total currents. The second solution was a potassium gluconate-based solution containing only approximately 14 mmol l^{-1} Cl^-, a concentration that is close to physiological for these muscle fibres (Bretag, 1987). The current-clamp results for both solutions were indistinguishable, apart from a slight slowing of the kinetics when recording with the low Cl^- solution. This is likely due to a smaller rate of change of voltage with time as a consequence of smaller current injections into the fibres compared with results using the high Cl^- solutions. In all experiments, background current was injected to control the ‘resting’ membrane potential to around –70 mV, a value that has been reported as the average resting membrane potential of larval inner, muscle fibres (Buss and Drapeau, 2000). In all inner muscle fibres recorded (*N*=15 in Normal solution and *N*=5 in low Cl^-), the injection of

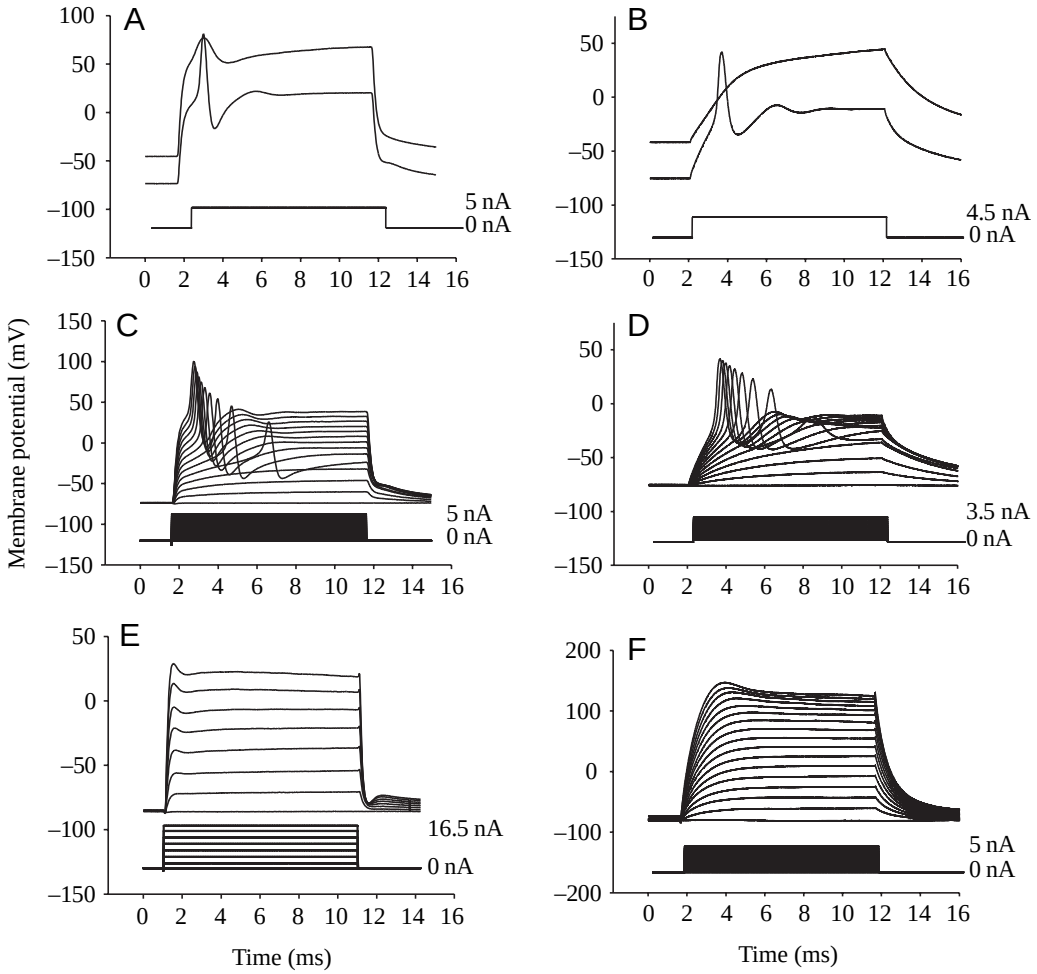

Fig. 7. Action potentials recorded in 4–6 d.p.f. zebrafish inner and outer muscle. (A,B) Action potentials were recorded from inner muscle fibres under current-clamp conditions in response to the injection of depolarizing current when the fibre was previously held at –70 mV (*N*=15). However, when the same depolarizing current was injected after holding the fibre at –45 mV, the evoked spike was considerably attenuated. Increasing the amplitude of the depolarizing current did not restore spike shape (data not shown). (A) Normal solution, (B) low Cl^- in the pipette-filling solution (*N*=5). (C,D) Applying 10 ms depolarizing pulses of increasing amplitude from a 'resting' membrane potential of around –70 mV never evoked more than one spike (*N*=10) in (C) Normal solution and (D) with low Cl^- in the pipette-filling solution (*N*=5). (E,F) In contrast to inner muscle fibres, depolarization of outer muscle fibres never elicited an action potential (*N*=5) in (E) Normal solution and (F) with low Cl^- in the pipette-filling solution (*N*=5).

depolarizing current resulted in one, and only one, action potential if the 'resting' potential was sufficiently negative (Fig. 7A,B). Injection of depolarizing current above a threshold value (which varied from cell to cell) resulted in an overshooting action potential, whereas the same depolarizing current applied to a background 'resting' potential of approximately –45 mV evoked a highly attenuated spike. No action potentials could be evoked by any current applied to outer muscle fibres (Fig. 7E,F; *N*=5 in Normal solution; *N*=6 in low Cl^-), even when the background, 'resting' potential was set to –100 mV (data not shown).

Progressively increasing the amplitude of the depolarizing current failed to elicit more than one action potential from inner muscle fibres (Fig. 7C,D; *N*=10 for Normal solution and *N*=5 for low Cl^-). A second action potential could, however, be elicited by applying two depolarizing pulses separated by an interval of at least 25 ms (Fig. 8A,B). When hyperpolarizing current was injected during the interstimulus interval, the minimum interval for which spiking could be evoked was around 0.5 ms (Fig. 8C,D; *N*=10 in Normal solution; *N*=5 for low Cl^-).

Discussion

Here we describe, for the first time, the steady-state properties of Na^+ and K^+ currents in larval, zebrafish trunk musculature. We also demonstrate that inner and outer muscle fibres of 4–6 d.p.f. zebrafish larva differ significantly in their electrical phenotypes. Outer muscle fibres appear to have very few inward currents and have a set of outward currents that show little or no inactivation. Furthermore, they are unable to support regenerative action potentials. Inner muscle fibres, in

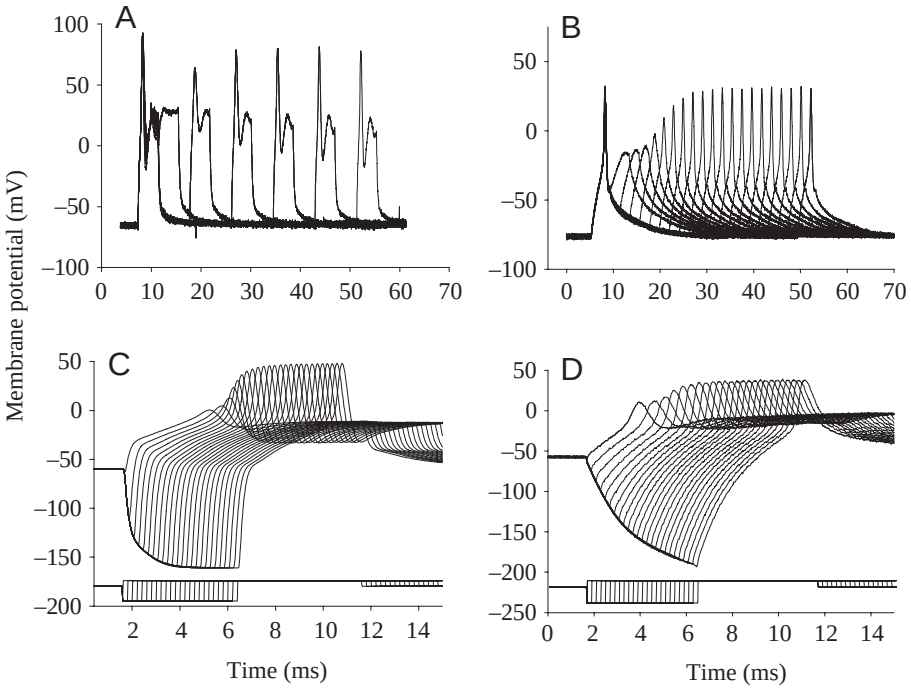

Fig. 8. Action potentials recorded in 4–6 d.p.f. zebrafish inner muscle. (A,B) Although no amount of depolarization of the inner muscle was found to elicit more than one spike, further spiking could be elicited in response to a second depolarization following a brief (>25 ms) return to the 'resting' potential in (A) Normal solution and (B) low Cl^- solution. (C,D) The minimal interstimulus interval required to elicit a second spike was greatly diminished by hyperpolarizing the membrane between stimuli. The recovery of the action potential was graded rather than all-or-none. (C) Normal solution, (D) in low Cl^- solution.

contrast, possess both robust inward and outward currents and are capable of supporting robust action potentials. The ability of outer muscle fibres to contract in the presence of 10 mmol l^{-1} BAPTA, coupled with the absence of inward currents, both features in contrast to inner muscle, suggest that the two muscle types use different excitation–contraction coupling mechanisms. This may be an adaptation of outer muscle, which is of the red type, to sustained, aerobic activity, whereas the inner muscle, of the white type, is adapted to sporadic escape-type activity (Greer-Walker and Pull, 1975; Van Raamsdonk et al., 1979, 1987). In addition, the triad structure in red muscle is reported to be quite varied, and poorly developed (Peachey and Huxley, 1962; Peachey, 1965) compared to white muscle.

The use of whole-cell patch in the current-clamp mode suffers from two experimental disadvantages: (1) the use of these headstages can distort the action potential waveform significantly, and (2) the intracellular environment is changed by dialysis with the pipette contents. We cannot therefore draw confident conclusions on the shape of the action potentials recorded in these experiments. It seems unlikely, however, that the phenomenon of once-only firing, which has also been observed in recordings from muscle fibres using sharp intracellular electrodes (Adrian and Bryant, 1974; Bryant 1962), is an artefact of the amplifier's circuitry, and so our findings provide confirmation that this phenomenon also occurs in zebrafish. Further, we cannot exclude the possibility that the inclusion of BAPTA in pipette-filling media may have altered the properties of ion channels through interference with calcium-dependent signalling pathways. We used the same pipette solutions in both current-clamp and voltage-clamp experiments, and since once-only firing is seen in our experiments as well as in those using sharp microelectrodes, it is unlikely that dialysis has greatly changed the properties of the channels that contribute to the firing pattern, although we cannot exclude the possibility that dialysis might have effected subtle alterations in channel properties.

The steady state and kinetic properties of skeletal muscle Na^+ channels have been investigated in a variety of preparations including humans (Almers et al., 1984), the rat (Duval and Leoty, 1978; Ruff et al., 1987; Moczydlowski et al., 1986), mouse (Gonoi et al., 1989), frog (Campbell and Hille, 1976) and elasmobranch fish (Stanfield, 1972). In addition, skeletal muscle Na^+ channels from rat have been cloned and sequenced (Trimmer et al., 1989; Kallen et al., 1990). In comparison to some of these previous studies, our estimated V_{50} of activation of the Na^+- currents in zebrafish fast-twitch muscle (of –7 mV) is notably more positive than that found in these other preparations, although the half-inactivation voltage in zebrafish white muscle (–74 mV) is very similar to previously published values (O'Leary, 1998), which range from –70 to –94 mV, with the vast majority falling between –70 and –76 mV. Many studies also report an outward K^+-current associated with fast-twitch muscle with properties similar to an A-current (Conor and Stevens, 1971a), in that it peaks and then inactivates with variable time courses (Adrian et al., 1970; Duval and Leoty, 1978; Stanfield, 1972; Vázquez, 1998).

Our finding that inner muscle is capable of supporting action potentials, is in contrast to the findings of Buss and Drapeau (2000), who were unable to evoke spikes from either red (outer) or white (inner) fibres. We show here that spikes evoked from a more depolarized resting membrane potential are highly attenuated. Buss and Drapeau (2000) report a resting membrane potential of –78 mV in 1-day embryos, to –71 mV in 6-day larvae, both values within the range over which we

were able to elicit spikes. In our hands we found the outer, red muscle incapable of supporting action potentials, similar to larval (Buss and Drapeau, 2000) and adult zebrafish preparations (Westerfield et al., 1986). The red muscle in other preparations, however, has been shown to support action potentials (Takeuchi, 1959; Stanfield, 1972), but these instances were rare, and to the best of our knowledge the majority of red fibres lack the ability to produce spikes.

The kinetic and steady state properties of the Na^+ and K^+ currents of inner muscle fibres are adapted to the behavioural functions of these muscles. Although inner muscle, in response to depolarization, produces a single, large action potential without the development of spike trains, it is nonetheless capable of following a train of depolarizing inputs at around 35 cycles per second (Buss and Drapeau, 2001). The inability of these muscles to produce spike trains could possibly serve as a safeguard against the depolarization accompanying one phase of the swimming cycle from evoking either tetany or a train of spikes, so ensuring strictly one spike per swim cycle. Earlier work suggested that a relatively high-density chloride shunt conductance may be responsible for the once-only firing in fast-twitch muscle (Adrian and Bryant, 1974; Bryant 1962), which is suggested to maintain the membrane potential at a hyperpolarized level following a spike. Our results show that white fibres are able to support once-only firing when filled with either a high (~140 mmol l^{-1} Cl^-) or a low (~14 mmol l^{-1} Cl^-) Cl^- solution, whilst red fibres are unable to support action potentials. We found that when recording with the low Cl^- solution we had to inject less current into both white and red fibres in order to depolarize them, compared with the high Cl^- solutions. Even though red fibres were only injected with ~5 nA of current, they depolarized to values approaching +150 mV, and further stimulation appears unlikely to produce spikes at such highly unphysiological potentials.

An alternative explanation for once-only firing might lie in the steady-state inactivation and voltage dependence of recovery from inactivation of the Na^+ current and the presence of the A-type K^+ currents. Sharp microelectrode studies of adult white fibres reported an average resting membrane potential of –81±8 mV (Westerfield et al., 1986), and more recent work on larval white fibres indicates a resting potential of approximately –71 mV, near to the value we assume in our current-clamp experiments. Our data indicate that at –71 mV, the reported value of the resting potential in larval white muscle (Buss and Drapeau, 2000), some 30% of the Na^+ channels are inactivated (Fig. 3). It is therefore possible that Na^+ channel inactivation is the likely explanation for the graded attenuation of action potentials upon background membrane depolarization (Fig. 7A,B). This in turn may provide a mechanism to prevent spike trains, since the steep voltage dependence of the rate of recovery from inactivation makes the relative refractory period dependent upon interspike hyperpolarization. This would effectively make high frequency firing conditional upon interspike repolarization. The role of the A current might accordingly be to ensure an interspike hyperpolarization. At the reported resting membrane potentials for zebrafish larval muscle, none of the K^+ channels would be activated and almost none inactivated, providing further reason for anticipating that these currents play a role in hastening repolarization. A role in producing slow, non-zero firing, as suggested by Connor and Stevens (1971b), is unlikely, since such firing is not expected in this muscle, which is rather associated with rapid swimming (Buss and Drapeau, 2002).

Thus, the kinetic and steady-state properties of the Na^+ and K^+ currents of inner muscle underlie a phenotype that permits high frequency firing in response to pulsatile depolarizing inputs of the kind expected during fast swimming, whilst safeguarding against the danger of tetanic spike trains in response to a single, strong depolarization, so permitting a large safety factor.

These predictions await further testing, either directly using manipulations that alter the ionic current properties, or indirectly using computer modeling. Thus, the larval zebrafish provides a particularly convenient model in which to trace behavioural adaptations in a motor system to molecular properties of ion channels.

This work was supported by an operating grant from the Natural Sciences and Engineering Research Council of Canada (NSERC) (to D.W.A.), and by an infrastructure grant from the Canadian Foundation for Innovation (CFI) (to D.W.A.).

References

Adrian, R. H. and Marshall, M. W. (1977). Sodium currents in mammalian muscle. *J. Physiol.* **268**, 223-250.

Adrian, R. H. and Bryant, S. H. (1974). On the repetitive discharge in myotonic muscle fibres. *J. Physiol.* **240**, 505-515.

Adrian, R. H., Chandler, W. K. and Hodgkin, A. L. (1970). Voltage clamp experiments in striated muscle fibres. *J. Physiol.* **208**, 607-644.

Almers, W., Roberts, W. M. and Ruff, R. L. (1984). Voltage clamp of rat and human skeletal muscles: measurements with an improved loose-patch clamp technique. *J. Physiol.* **347**, 751-768.

Armstrong, C. M. and Hille, B. (1998). Voltage-gated ion channels and electrical excitability. *Neuron* **20**, 371-380.

Bretag, A. H. (1987). Muscle chloride channels. *Physiol. Rev.* **67**, 618-724.

Bryant, S. H. (1962). Muscle membrane of normal and myotonic goats in normal and low external chloride. *Fedn. Proc.* **21**, 312.

Buss, R. R. and Drapeau, P. (2000). Physiological properties of zebrafish embryonic red and white muscle fibers during early development. *J. Neurophysiol.* **84**, 1545-1557.

Buss, R. R. and Drapeau, P. (2001). Synaptic drive to motoneurons during fictive swimming in the developing zebrafish. *J. Neurophysiol.* **86**, 197-210.

Buss, R. R. and Drapeau, P. (2002). Activation of embryonic red and white muscle fibers during fictive swimming in the developing zebrafish. *J. Neurophysiol.* **87**, 1244-1251.

Camacho, J., Delay, M. J., Vazquez, M., Argüello, C. and Sánchez, J. A. (1996). Transient outward K^+ channels in vesicles derived from frog skeletal muscle plasma membranes. *Biophys. J.* **71**, 171-181.

Campbell, D. T. and Hille, B. (1976). Kinetic and pharmacological properties of the sodium channel of frog skeletal muscle. *J. Gen. Physiol.* **67**, 309-323.

Catterall, W. A. (1992). Cellular and molecular biology of voltage-gated sodium channels. *Physiol. Rev.* **72**, S15-S48.

Connor, J. A. and Stevens, C. F. (1971a). Inward and delayed outward membrane currents in isolated neural somata under voltage clamp. *J. Physiol.* **213**, 1-19.

Connor, J. A. and Stevens, C. F. (1971b). Prediction of repetitive firing behaviour from voltage clamp data on an isolated neurone soma. *J. Physiol.* **213**, 31-53.

Cruz, L. J., Gray, W. R., Olivera, B. M., Zeikus, R. D., Kerr, L., Yoshikami, D. and Moczydlowski, E. (1985). Conus geographus toxins that discriminate between neuronal and muscle sodium channels. *J. Biol. Chem.* **260**, 9280-9288.

Drapeau, P., Saint-Amant, L., Buss, R. R., Chong, M., McDearmid, J. R. and Brustein, E. (2002). Development of the locomotor network in zebrafish. *Prog. Neurobiol.* **68**, 85-111.

Duval, A. and Leoty, C. (1978). Ionic currents in mammalian fast skeletal muscle. *J. Physiol.* **278**, 403-423.

Duval, A. and Leoty, C. (1980a). Ionic currents in slow twitch skeletal muscle in the rat. *J. Physiol.* **307**, 23-41.

Duval, A. and Leoty, C. (1980b). Comparison between the delayed outward current in slow and fast twitch skeletal muscle in the rat. *J. Physiol.* **484**, 313-329.

Goldin, A. L. (2001). Resurgence of sodium channel research. *Annu. Rev. Physiol.* **63**, 871-894.

Gonoi, T., Hagihara, Y., Kobayashi, J., Nakamura, H. and Ohizumi, Y. (1989). Geographutoxin-sensitive and insensitive sodium currents in mouse skeletal muscle developing in situ. *J. Physiol.* **414**, 159-177.

Greer-Walker, M. and Pull, G. A. (1975). A survey of red and white muscle in marine fish. *J. Fish Biol.* **7**, 295-300.

Hamill, O. P., Marty, A., Neher, E., Sakmann, B. and Sigworth, F. J. (1981). Improved patch-clamp techniques for high-resolution current recording from cells and cell-free membrane patches. *Pflug. Arch.* **391**, 85-100.

Hille, B. (2001). *Ion Channels Of Excitable Membranes*. Sunderland, MA USA: Sinauer Associates Inc.

Isom, L. L., Scheuer, T., Brownstein, A. B., Ragsdale, D. A., Murphy, B. J. and Catterall, W. A. (1995). Functional co-expression of the α1 and type IIA α subunits of sodium channels in a mammalian cell line. *J. Biol. Chem.* **270**, 3306-3312.

Kallen, R. G., Sheng, Z-H., Yang, J., Chen, L., Rogart, R. B. and Barchi, R. L. (1990). Primary structure and expression of a sodium channel characteristic of denervated and immature rat skeletal muscle. *Neuron* **4**, 233-242.

Lerche, H., Mitrovic, N., Dubowitz, V. and Lehmann-Horn, F. (1996). Paramyotonia congenital: the R1448P Na^+ channel mutation in adult human skeletal muscle. *Ann. Neurol.* **39**, 599-608.

Magistretti, J., Mantegazza, M., Guatteo, E. and Wanke, E. (1996). Action potentials recorded with patch-clamp amplifiers: are they genuine? *Trends Neurosci.* **19**, 530-534.

Moczydlowski, E., Olivera, B. M., Gray, W. R. and Strichartz, G. R. (1986). Discrimination of muscle and neuronal Na-channel subtypes by binding competition between [^{3}H]saxitoxin and ω-conotoxins. *Proc. Natl. Acad. Sci. USA* **83**, 5321-5325.

Nguyen, P. V., Aniksztejn, L., Catarsi, S. and Drapeau, P. (1999). Neuromuscular transmission during early development of the zebrafish. *J. Neurophysiol.* **81**, 2852-2861.

O'Leary, M. E. (1998). Characterization of the isoform-specific differences in the gating of neuronal and muscle sodium channels. *Can. J. Physiol.* **76**, 1041-1050.

Peachey, L. D. (1965). The sarcoplasmic reticulum and transverse tubules of the frog's sartorius. *J. Cell Biol.* **25**, 209-231.

Peachey, L. D. and Huxley, A. F. (1962). Structural identification of twitch and slow striated muscle fibres of the frog. *J. Cell Biol.* **13**, 177-180.

Penner, R. (1995). A practical guide to patch clamping. In *Single-Channel Recording* (ed. B. Sakmann and E. Neher), pp. 3-28. New York: Plenum Press.

Plaut, I. (2000). Effects of fin size on swimming performance, swimming behaviour and routine activity of zebrafish *Danio rerio*. *J. Exp. Biol.* **203**, 813-820.

Ruff, R. L. (1996). Channel slow inactivation and the distribution of sodium channels on the skeletal muscle fibers enable the performance properties of different skeletal muscle fiber types. *Acta Physiol. Scand.* **156**, 159-168.

Ruff, R. L., Simoncini, L. and Stühmer, W. (1987). Comparison between slow sodium channel inactivation in rat slow- and fast-twitch muscle. *J. Physiol.* **383**, 339-348.

Saint-Amant, L. and Drapeau, P. (1998). Time course of the development of motor behaviors in the zebrafish embryo. *J. Neurobiol.* **37**, 622-632.

Saint-Amant, L. and Drapeau, P. (2000). Motoneuron activity patterns related to the earliest behavior of the zebrafish embryo. *J. Neurosci.* **20**, 3964-3972.

Sanes, J. R. and Lichtman, J. W. (1999). Development of the vertebrate neuromuscular junction. *Annu. Rev. Neurosci.* **22**, 389-442.

Stanfield, P. R. (1972). Electrical properties of white and red muscle fibres of the elasmobranch fish *Scyliorhinus canicula*. *J. Physiol.* **222**, 161-186.

Takeuchi, A. (1959). Neuromuscular transmission of fish skeletal muscles investigated with intracellular microelectrode. *J. Cell. Comp. Physiol.* **54**, 211-221.

Trimmer, J. S., Cooperman, S. S., Tomiko, S. A., Zhou, J., Crean, S. M., Boyle, M. B., Kallen, R. G., Sheng, Z., Barchi, R. L., Sigworth, F. J. et al. (1989). Primary structure and functional expression of a mammalian skeletal muscle sodium channel. *Neuron* **3**, 33-49.

Van Raamsdonk, W., Moss, W., Tekronnie, G., Pool, C. W. and Mijzen, P. (1979). Differentiation of the musculature of the teleost *Brachydanio rerio*. II. Effects of immobilization on the shape and structure of somites. *Acta Morphol. Neerl-Scand.* **17**, 259-274.

Van Raamsdonk, W., Smit-Onel, M., Scholten, G., Hemrika, W. and Robbe, B. (1987). Metabolic specialization of spinal neurons and the myotomal muscle in post-hatching stages of the zebrafish, *Brachydanio rerio. Z. Mikrosk-Anat. Forsch.* **101**, 318-330.

Vázquez, M. (1998). Single-channel analysis of fast transient outward K^+ currents in frog skeletal muscle. *Pflug. Arch.* **436**, 95-103.

Westerfield, M., McMurray, J. V. and Eisen, J. S. (1986). Identified motoneurons and their innervation of axial muscles in the zebrafish. *J. Neurosci.* **6**, 2267-2277.

Westerfield, M. (1995). *The Zebrafish Book: A guide for the laboratory use of zebrafish (*Brachydanio rerio*)*. Eugene, OR: University of Oregon Press.